Autonomous Mobility & Manipulation of a 9-DoF WMRA

W. Pence, F. Farelo, Y. Sun, R. Alqasemi, and R. Dubey

***Abstract*—Two prototypes of a 9-DoF wheelchair-mounted robotic arm (WMRA) have been developed as assistive devices, consisting of a 7-DoF robotic arm and a 2-DoF power wheelchair. Combined kinematics and redundancy resolution have been previously implemented. In this work, we focus on control methods to allow autonomous mobility and manipulation for the execution of activities of daily living (ADL). Results of physical testing are also presented.**

Keywords-WMRA; ADL; rehabilitation; visual servoing.

I. INTRODUCTION

The 2010 US Census Bureau report on disability shows that about 10 percent of the working age population has a disability, and there exists a great disparity among the employment-to-population ratio for disabled citizens [1]. For those with upper body disabilities, it has been shown that robotic arms can be used as effective assistive devices [2]. Two prototypes of a 9-DoF wheelchair-mounted robotic arm (WMRA) have been developed, which outperform WMRAs using commercially-available arms [3, 4]. Interfaces for the WMRA consist of the P300 brain-computer interface [5], 3D joystick, touchscreen, voice recognition, and eye gaze [6]. Details on the control system of the 9-DoF WMRA can be reviewed in [3, 4, 5]. Redundancy of the additional DoFs is accomplished using weighted least-norm solution with singularity-robust pseudo inverse [7]. Combination of the robotic arm and wheelchair kinematics is done using Jacobian augmentation [8]. The 2-DoF of the power wheelchair consist of linear translation and rotation around the vertical axis.

In [3], an optimized redundancy resolution algorithm was implemented to provide a platform for autonomous execution of activities of daily living (ADL). However, for many ADL tasks it is necessary to generate separate trajectories for the mobile platform and manipulator. This way the wheelchair can be positioned such that specialized ADL tasks can take place. Dual-trajectory control was recently used to implement a "Go to and open the door" task described in [9]. For the physical implementation of dual-trajectory control, it is desirable to integrate visual servoing to track the goal object in real time. In this work, we implement vision-based dual-trajectory control to physically execute a basic "Go To and Pick Up" ADL task in a real-world environment and provide results from this testing. It should be noted that although the WMRA applies specifically to the application of rehabilitation, these concepts can be extended to general purpose mobile manipulators.

This work was supported in part by the National Science Foundation (NSF) under Grant IIS-0713560.

Figure 1. Monocular eye in hand camera mounted on the gripper.

II. CONTROL SYSTEMS

A. Vision-Based Control

Visual servoing [14] has been implemented with various commercially-available robotic arms to guide the end effector towards a goal as in [10, 11, 12]. Using image-based visual servoing (IBVS), the end effector can be guided toward the goal object using 2D coordinates during the execution of an ADL. Vision-based systems allow much of the control to be automated, resulting in easier execution of the ADL by the user. Vision-based approaches can handle dynamic environments with moving objects, and are also able to overcome imprecision of physical hardware.

We use an eye in hand camera on the end effector for an IBVS technique. Figure 1 shows the gripper with a standard monocular camera fitted. After the goal object has been selected, it is tracked in the image plane using Continuously Adaptive Mean Shift (camshift) implemented in the OpenCV computer vision library [13]. The basic goal of visual servoing is to minimize an error given by:

$$e(t) = s(m(t),a) - s^* \quad (1)$$

where $s(m(t),a)$ is the set of current measurements extracted from the camera image and s^* is the set of desired values. For our application, $s(m(t),a)$ consists of the current location of the 2-dimensional centroid of the goal object in the image plane. Since our task is to grasp the goal object, we desire to manipulate the system such that the goal object is in the center of the image plane of the eye in hand camera. Therefore when we approach the goal object, it will be positioned between the gripper paddles of the end effector. In this case, s^* is the 2-dimensional center of the image plane. Based on the 2-dimensional camera frame, $e_x(t)$ and $e_y(t)$ are calculated in the x-direction and y-direction, respectively, with respect to the camera frame. We use these error values to modify the velocities for movements in the y-direction and z-direction, respectively, with respect to the wheelchair frame. Therefore,

when the system has approached and centered on the goal object and *e(t)* is minimized, velocity reaches zero.

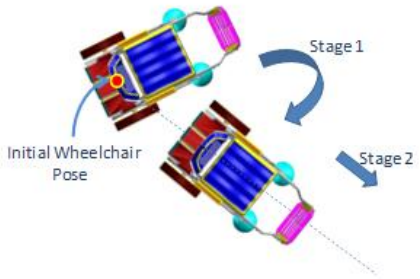

Figure 2. Our case of the two stages for the secondary trajectory to be followed by the wheelchair.

B. Dual-Trajectory Control

During autonomous execution of an ADL, the WMRA control system provides a set of trajectories for the end effector to follow. In this case, the wheelchair and end effector follow the same trajectory. However, for some ADLs it may be necessary that the wheelchair follow a second set of trajectories. Optimized dual-trajectory control of the WMRA is detailed in [9]. The secondary trajectory of the wheelchair can be divided into three stages: orient the wheelchair to face its desired goal, proceed with a linear motion along the secondary trajectory to approach the final planar coordinates, and finally orient the wheelchair to its final desired orientation. The three stages can be visualized in Figure 2. Next, we describe criteria functions that provide the secondary trajectory for the mobile platform using vision-guided control.

C. Criteria Functions for Weighted Optimization

Criteria functions for weighted optimization of the 7-DoF arm can be reviewed in [3, 4, 5]. These optimizations allow the manipulator to overcome singularities, joint limits, and workspace limitations. For the 2-DoF wheelchair, criteria functions can be defined for each stage of the trajectory based on the desired motion of the wheelchair. Mathematical representations can be obtained by treating the range of desired wheelchair motion as a motion limit. These mathematical representations can be reviewed in [15].

The diagonal weight matrix *W* for the 9-DoF system is a 9x9 matrix (2) that is multiplied with the Jacobian to modify mobility and manipulation.

$$W = \begin{bmatrix} w_1 + \left|\frac{\partial H(q)}{\partial q_1}\right| & 0 & \cdots & \cdots & 0 \\ 0 & w_2 + \left|\frac{\partial H(q)}{\partial q_2}\right| & 0 & \cdots & 0 \\ \vdots & 0 & \ddots & \cdots & \vdots \\ \vdots & \vdots & \vdots & w_X & 0 \\ 0 & 0 & \cdots & 0 & w_\phi \end{bmatrix} \quad (2)$$

Weights w_1 through w_7 are user-set preference values for each DoF of the arm and also carry joint limit avoidance functions. For the 2-DoF of the wheelchair, w_x is the weight optimization for the wheelchair translation, and w_φ is the weight optimization for the wheelchair rotation about its vertical axis. We must define criteria functions to compute w_x and w_φ for each stage of motion. For our example "Go To and Pick Up" task, we only define criteria functions for two stages of dual-trajectory control. When the wheelchair has approached the goal object, no further orientation in Stage 3 is necessary since it will already be in the desired orientation.

For the first stage of motion, we have:

$$w_\phi = \frac{4\cdot(e_{\max} - e_{current})^2 \cdot (e_{current} - e_{\min})^2}{(e_{\max} - e_{\min})^2 \cdot (2\cdot e_{current} - e_{\max} - e_{\min})} \quad (3)$$
$$w_x \to \infty$$

where $e_{\max}$ is the maximum possible error *e(t)* from (1), $e_{\min}$ is the desired error, and e_{current} is the current error from the image measurements. In our case, $e_{\max}$ is set to half of the image plane width, which would be the maximum possible error. We seek to minimize the error, so $e_{\min}$ is set to zero. To determine e_{current}, we use the $e_x(t)$ equation described in (1) to compute the current visual error. During the first stage, we wish to rotate the mobile platform so that it faces the goal object. We compute w_φ based on the described values, and set w_x to infinity since no translation is necessary during this stage. We also set w_1 through w_7 to infinity since no arm movement is necessary during this stage.

For the second stage of motion, we have:

$$w_\phi \to \infty$$
$$w_x = \frac{4\cdot(X_{\max} - X_{current})^2 \cdot (X_{current} - X_{\min})^2}{(X_{\max} - X_{\min})^2 \cdot (2\cdot X_{current} - X_{\max} - X_{\min})} \quad (4)$$

where *X* relates to the linear movement of the wheelchair. We can determine the distance to the goal object using proximity sensors. Therefore we can set the variables relating to *X* accordingly. During the second stage, we wish to translate the mobile platform straight forward to approach the goal object. We compute w_x based on distance information, and set w_φ to infinity since no rotation is necessary during this stage. We set w_1 through w_7 to one since we desire to have the arm to center on the goal object using $e_x(t)$ and $e_y(t)$ during this stage.

These criteria functions allow us to generate a secondary trajectory for the wheelchair during autonomous execution of ADL tasks.

D. Collision Avoidnace and Sensor Fusing

During motion of the wheelchair, it is important to provide a collision avoidance system in case obstacles are encountered during autonomous motion. We are using a monocular eye in hand camera for visual servoing tasks, but we can also use a stereoscopic Point Grey Bumblebee camera, which can compute distance information using the generated disparity map. We use an array of 12 Sharp GP2Y0A21YK0F infrared LED proximity sensors along with 2 Parallax PING ultrasonic sonar proximity sensors. Infrared proximity sensors can be unreliable with glossy or clear surfaces, sonar proximity sensors can be unreliable with soft surfaces, and stereoscopic

disparity information can be noisy for surfaces with poor texture. For these reasons, it is important to have a reliable sensing system that works well with many different environments.

All of these sensing systems are fused together to provide reliable sensor data for various surfaces and environments. This is done by calibrating the distance information between the physical proximity sensors and the stereoscopic disparity maps. We focus on the fused sensor zones visualized in Figure 3. Since we are mainly concerned with forward motion of the wheelchair, we focus on the forward-facing sensor zones. To provide collision avoidance, we implemented a basic occupancy grid technique [16] to detect obstacles, override the autonomous control to navigate around the obstacle, and finally continue vision-based control to reach the target.

E. Physical Implementations

The wheelchair system has been modified using a Lab Jack device in order to control motion with a PC. A monocular eye in hand camera is mounted on the end effector for visual servoing control. Proximity sensors on the WMRA system allow for a collision avoidance system.

To explain how the system operates, we consider a simple "Go To and Pick Up" ADL task, seen in Figure 4. The user is provided a view of the workspace as seen from the eye in hand camera and selects a goal object. OpenCV camshift then tracks the object in real-time and *e(t)* is computed from (1). Initially, the platform moves according to the weights computed from (3) during the first stage, where the wheelchair rotates to face the desired goal. Figure 5 shows the physical errors computed during the first stage. During the second stage, the weights computed in (4) move the wheelchair linearly toward the goal object. Simultaneously, the arm centers on the goal object using Cartesian control based on the wheelchair coordinate frame. When the goal object is within the gripper paddles, the system stops and the gripper paddles are closed to grasp the object. The grasped object is then delivered to the user by means of preprogrammed position control. Figure 6 shows the physical errors computed during the entire execution from beginning to end.

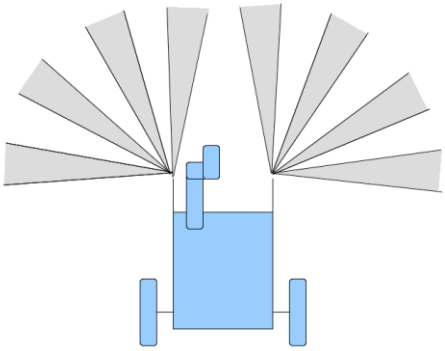

Figure 3. Forward-facing sensor zones.

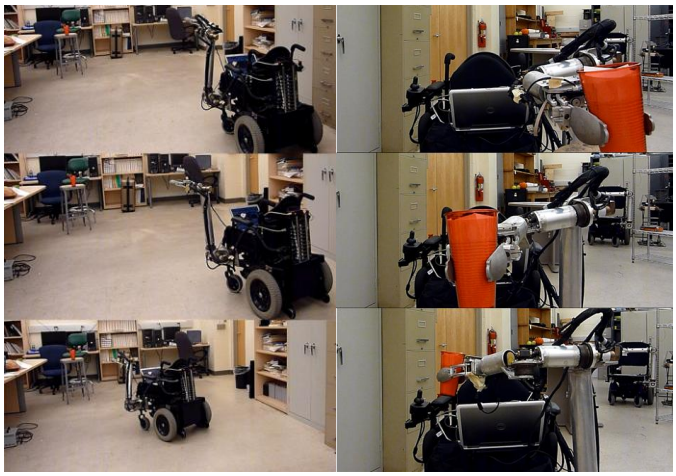

Figure 4. Execution of a "Go To and Pick Up" task for a red cup.

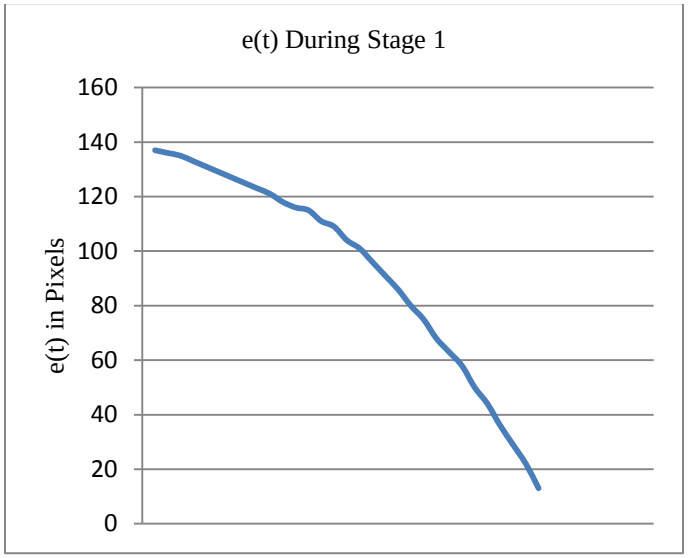

Figure 5. Error in pixels versus time for the first stage.

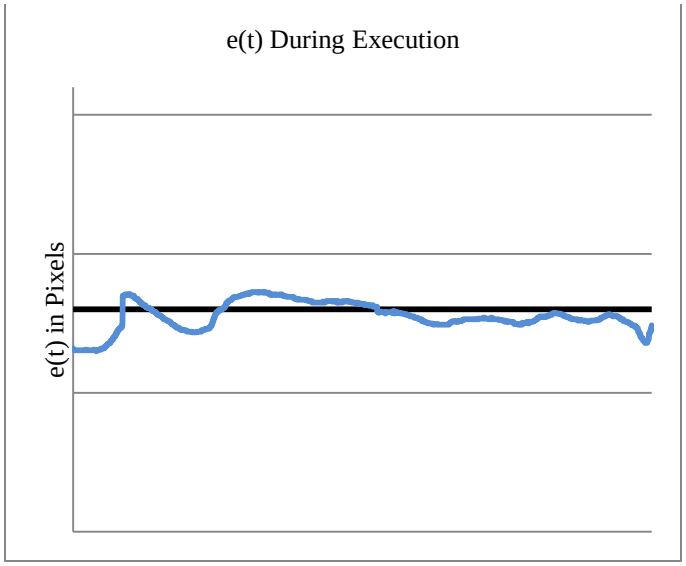

Figure 6. Error in pixels over time for the entire task execution.

III. Conclusions and Future Work

Various ADL tasks can be executed autonomously using the control methods implemented. These methods have been implemented on the 9-DoF WMRA and we have executed a "Go To and Pick Up" task using the physical WMRA. Future work includes physical implementation of position-based visual servoing (PBVS) along with object detection in order to determine object pose to grasp objects of various classes. While the 2-dimensional IBVS approach allows us to approach the object with the WMRA, we also need a system that can determine object pose so that we can manipulate the 7-DoF robotic arm to grasp the goal object. We can use PBVS to determine object pose based on the 3-dimensional vision data. Using an object detection technique such as scale invariant feature transform (SIFT) [17], we can detect objects of interest using feature keypoints stored in a database. By matching the features between the real-time image and the goal orientation from the database, we can execute a similar visual servoing technique so that the error in all 6-DoF is minimized and the object is ready to be grasped from any orientation.

A more advanced graphical user interface (GUI) is also being developed that will provide a pool of ADL tasks for the detected object. This GUI will be especially designed to work with the BCI and eye gaze interfaces.

Acknowledgment

We would like to thank the members of the Center for Assistive, Rehabilitative and Robotics Technologies (CARRT) for their support relating to the WMRA project, especially Paul Mitzlaff for handling the electrical and mechanical aspects.

References

[1] US Census Bureau, "Disability Among the Working Age Population: 2008 and 2009," Census Brief, September 2010, http://www.census.gov/prod/2010pubs/acsbr09-12.pdf

[2] Reswick J.B., "The Moon over Dubrovnik - A Tale of Worldwide Impact on Persons with Disabilities," *Advances in External Control of Human Extremities*, 1990.

[3] R. Alqasemi and R. Dubey. "Maximizing Manipulation Capabilities for People with Disabilities Using a 9-DoF Wheelchair-Mounted Robotic Arm System," *Proceedings of the 2007 IEEE 10th International Conference on Rehabilitation Robotics*.

[4] P. Shrock, F. Farelo, R. Alqasemi and R. Dubey. "Design, Simulation and Testing of a New Modular Wheelchair Mounted Robotic Arm to Perform Activities of Daily Living," *Proceedings of the 2009 IEEE 11th International Conference on Rehabilitation Robotics*.

[5] M. Palankar, K. De Laurentis, R. Alqasemi, E. Veras, R. Dubey, Y. Arbel, and E. Donchin, "Control of a 9-DoF Wheelchair-Mounted Robotic Arm System using a P300 Brain Computer Interface: Initial Experiments," *Proceedings of IEEE International Conference on Robotics and Biomimetics*, pp. 348-353, February 2009.

[6] C. Bringes, J. Jones, M. Malek, B. Simons, W. Pence, and R. Alqasemi. *Human-Computer Interaction for the WMRA*, FCRAR 2011.

[7] Nakamura, Y., "Advanced robotics: redundancy and optimization," Addison- Wesley Publishing, 1991, ISBN 0201151987.

[8] A. Luca, G. Oriolo, and P. Giordano, "Kinematic Modeling and Redundancy Resolution for Nonholonomic Mobile Manipulators", Proceedings of the 2006 IEEE International Conference on Robotics and Automation (ICRA), pp. 1867-1873.

[9] F. Farelo, R. Alqasemi, and R. Dubey. "Optimized Dual-Trajectory Tracking Control of a 9-DoF WMRA System for ADL Tasks". Procedings of the 2010 IEEE International Conference on Robotics and Automation (ICRA).

[10] Driessen, B.; Liefhebber, F.; Kate, T.T.; Van Woerden, K.; , "Collaborative control of the MANUS manipulator," Rehabilitation Robotics, 2005. ICORR 2005. 9th International Conference on , vol., no., pp. 247- 251, 28 June-1 July 2005.

[11] Liefhebber, F.; Sijs, J.; , "Vision-based control of the Manus using SIFT," Rehabilitation Robotics, 2007. ICORR 2007. IEEE 10th International Conference on , vol., no., pp.854-861, 13-15 June 2007.

[12] Kim, Dae-Jin; Lovelett, Ryan; Behal, Aman; , "Eye-in-hand stereo visual servoing of an assistive robot arm in unstructured environments," Robotics and Automation, 2009. ICRA '09. IEEE International Conference on , vol., no., pp.2326-2331, 12-17 May 2009.

[13] G.R. Bradski, Computer video face tracking for use in a perceptual user interface, Intel Technology Journal, Q2 1998.

[14] Chaumette, F.; Hutchinson, S.; , "Visual servo control. I. Basic approaches," Robotics & Automation Magazine, IEEE , vol.13, no.4, pp.82-90, Dec. 2006.

[15] F. Farelo, W. Pence, R. Alqasemi, and R. Dubey, "WMRA Mobility & Manipulation Visual Servoing Control for the Performance of ADL Tasks," IROS 2011. "unpublished"

[16] Thrun, Sebastian, Wolfram Burgard and Dieter Fox. Probabilistic Robotics. The MIT Press: Cambridge, Massachusetts, 2005.

[17] Lowe, David. "Distinctive Image Features from Scale-Invariant Keypoints". International Journal of Computer Vision 2004.